Journal of Information Systems Engineering and Management
2025, 10(4)
e-ISSN: 2468-4376
https://www.jisem-journal.com/

Research Article

Enhancing DC and RF Performance of AlGaN/GaN HEMTs Using Delta-Doped Double Barriers and 4H-SiC Substrates

Djelti Fayssal[1], Ould Abbas Amaria [1], Abdelmalek Douara[2], Bechlaghem Fatima Zahra[1]

[1] *Abou Bakr Belkaid University of Tlemcen, Algeria, Department of Physics, Faculty of Sciences, Research Unit on Materials and Renewable Energies Tlemcen, 13000 Algeria,*

[2] *Faculty of Science and Technology, Tissemsilt University, Tissemsilt, 38000, Algeria*

Email: fdjeltiphd@gmail.com

ARTICLE INFO

Received:25 July 2025

Revised:01 Sept 2025

Accepted:08 Sept 2025

ABSTRACT

This study aims to enhance the direct current (DC) and radio-frequency (RF) performance of an AlGaN/GaN high electron mobility transistor (HEMT) employing a T-shaped gate structure. We propose a novel device architecture featuring a delta-doped double AlGaN barrier layer combined with a 4H-SiC substrate, leveraging its superior thermal conductivity and electrical properties. Device performance was evaluated using Silvaco TCAD simulation tools. The optimized design, incorporating a 4 nm thick delta-doped double AlGaN barrier, significantly improves electron mobility and device performance. Simulation results reveal a maximum drain current of 0.987 A and a peak transconductance of 698 mS/mm at a drain-source voltage of 3 V. Furthermore, the device demonstrates exceptional high-frequency performance, achieving a cut-off frequency (fT) of 748 GHz and a maximum oscillation frequency (fmax) of 1068.8 GHz. These results underscore the efficacy of the proposed delta-doped double barrier design and 4H-SiC substrate in enabling high-performance HEMTs for high-power and high-frequency applications.

Keywords: AlGaN/GaN; HEMT; 4H-SiC; Silvaco TCAD; Cut-off frequency.

INTRODUCTION

This study presents an in-depth analysis of AlGaN/GaN HEMTs, with a focus on strategies to optimize their electrical performance in direct current (DC) and radio frequency (RF). The integration of an ultra-reduced grid (0.02 µm), an AlN spacer layer, as well as Si_3N_4 surface passivation helps to mitigate short-channel effects and improve stability and current density. Numerical modeling is performed via Silvaco TCAD tools to evaluate the static and dynamic characteristics of the device, with the aim of meeting the requirements of high-power and high-frequency applications. High Electron Mobility Transistors (HEMTs), also known as Heterojunction Field Effect (HFET) transistors, are central to high-frequency applications due to their outstanding performance in power management and low noise. These properties make HEMTs one of the most promising and competitive technologies for a wide range of radio frequency (RF) circuits, including power amplifiers, oscillators, mixers, and wireless communication systems, including radar applications [1–4].

The HEMT is a field-effect device based on a heterostructure, operating from a PN junction mechanism. It typically has a region of type n highly doped and a region of p Lightly doped. In this configuration, electrons, the majority carriers, ensure the conduction of current [5–7]. One of the main characteristics of HEMTs is their high electronic mobility, resulting from a significant reduction in intra- and inter-band scattering phenomena. This reduction limits collisions between carriers, thus promoting rapid electron transport. In HEMTs based on nitrided materials, the structure is based on materials with a wide bandgap, such as gallium nitride (GaN), with a bandgap of 3.4 eV, and aluminum gallium nitride

(AlGaN), whose bandgap varies according to aluminum content, reaching up to 6.1 eV [8]. The heterojunction formed at the interface of these materials allows the generation of a two-dimensional electron gas (2DEG), induced by the effects of spontaneous polarization and piezoelectric polarization, as well as by band discontinuity. Electrons that are vertically confined, but free to move in the plane, exhibit high mobility, which directly influences essential parameters such as threshold voltage and transition frequency (fT) [9–12]. The integration of a back barrier into the HEMT structure helps to mitigate short-channel effects, including the reduction of the Drain-Induced Barrier Lowering (DIBL), while increasing the cut-off frequency [13, 14]. Compared to gallium arsenide (GaAs)-based devices, GaN HEMTs offer significant advantages, including higher breakdown voltage, higher power density, better thermal conductivity, as well as reliable operation in extreme and high-temperature environments. These advantages are directly related to the wider bandgap of GaN (3.4 eV vs. 1.4 eV for GaAs) [7, 15–17].

In order to improve electrical stability and limit surface leakage currents, a passivation layer is usually deposited on HEMT structures. Silicon nitride (Si_3N_4) is frequently used for this purpose. This layer also helps to minimize the impact of surface finishes and stabilize the electrical characteristics of the device. At the same time, careful engineering of the channel layer reduces the influence of traps in the buffer layer, often caused by crystalline misalignments or structural defects, which can affect carrier transport. The AlGaN barrier layer, located above the channel, plays a key role in the formation of 2DEG, but it is also sensitive to leakage currents, especially in high polarization regimes, which can lead to current instability and performance degradation [18–20]. To overcome these limitations, an aluminum nitride (AlN) spacer layer is interspersed between the AlGaN and GaN layers. Thanks to its high breakdown field and strong polarization field, AlN improves carrier confinement, reduces the effect of hot electrons, increases the leaf charge density, and thus contributes to better high-frequency, high-power performance [21, 22]. A heavily doped GaN cap layer is typically added to the top of the structure to optimize carrier injection and stabilize the operation of the device under high field. This cap acts as a charging reservoir, improving the current density and robustness of the component [23].

In this study, an advanced HEMT structure is proposed and analyzed, integrating an ultra-short-length grid of 0.02 μm as well as a 100 nm thick Si_3N_4 passivation layer. A complete characterization in direct current (DC) and radio frequency (RF) is performed, covering current-voltage characteristics, transconductance, cut-off frequency and noise performance. The objective is to evaluate the impact of the aggressive reduction of the gate length, coupled with optimized passivation, on the electrical performance of the device, both at low and high frequencies. This analysis contributes to improving the understanding of the behavior of HEMTs in the context of new technological constraints related to the miniaturization of components.

DEVICE STRUCTURE

The structure depicted in Fig. 1 illustrates a cross-sectional view of the proposed AlGaN/GaN high-electron-mobility transistor (HEMT) with a T-shaped gate. The nitride-based heterostructure comprises the following layers: a 32 nm AlN buffer layer, a 7 nm n-type GaN channel layer, a 1 nm AlGaN spacer layer, a second 1 nm AlGaN spacer layer, a 2 nm AlGaN donor layer doped with 5 × 1018 cm−3, a 3 nm $Al_{0.2}Ga_{0.8}N$ Schottky barrier layer, and a 2 nm GaN cap layer doped with 5 × 1018 cm−3. The proposed structure is grown on a 4H-SiC substrate. The source and drain electrodes are ohmic contacts, while the gate electrode employs a Schottky contact using gold, with a work function of 4.55 eV. Material parameters used in the simulations are detailed in Table 1.

Journal of Information Systems Engineering and Management
2025, 10(4)
e-ISSN: 2468-4376
https://www.jisem-journal.com/

Research Article

Table 1: Device Settings

Parameter	***VALUE***
Gate Length (L_G)	20 nm
Channel length	300 nm
Source Length (L_S)	50 nm
Drain Length (L_D)	50 nm
Gate Work Function	4.55 eV
Doping Concentration (GaN Channel)	8×10^{16} cm^{-3}
Doping Concentration (GaN Cap)	$8{\times}10^{19}$ per cm^{-3}

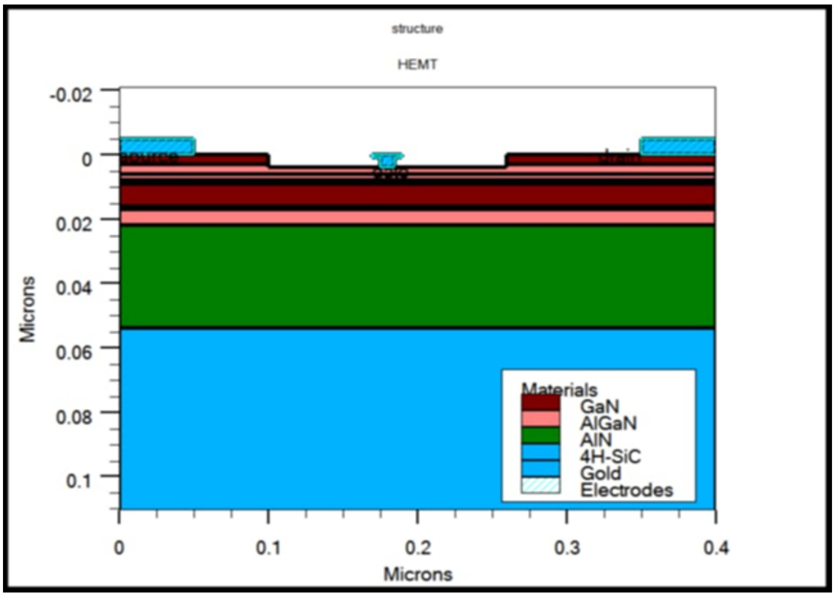

Figure 1: Schematic cross-section of the simulated T-shaped AlGaN/GaN HEMT.

SIMULATION RESULTS AND DISCUSSION

The electrical characteristics of the proposed AlGaN/GaN HEMT device were obtained by detailed numerical simulations using Silvaco's ATLAS device simulator. The simulation framework integrates multiple physical models to accurately capture the transport and recombination mechanisms within the semiconductor structure. To account for carrier recombination effects, the Shockley-Read-Hall (SRH) recombination model was used [24][25]. This model is essential for simulating non-radiative recombination processes due to defects or trap states in the bandgap, especially those associated with

Journal of Information Systems Engineering and Management
2025, 10(4)
e-ISSN: 2468-4376
https://www.jisem-journal.com/
Research Article

phonon-assisted transitions. These effects are essential for determining leakage currents and out-of-state behavior, especially in materials with a wide bandgap such as GaN.

E-mobility was modeled using Albrecht's low-field mobility model, which provides a more accurate estimate of carrier mobility under low electric field conditions [26]. This model takes into account various scattering mechanisms, including impurity, phonon and dislocation scattering, key factors in the performance of high electron mobility transistors (HEMTs).

Newton's iterative method was used to solve the coupled equations of semiconductors and extract key terminal features such as drain current, drain voltage, and gate voltage. This method ensures numerical stability and convergence when simulating nonlinear semiconductor behaviors [27].

In the bias condition VGS = 0 V and VDS = 0.6 V, the proposed device achieved a maximum drain current ID,max of approximately 0.987 A, indicating a high current control capability. Figure 2 illustrates the family of output characteristics obtained at different gate-to-source voltages. In this simulation, the drain voltage was swept from 0 V to 3 V in steps, while the gate voltage was modified to observe the switching behavior of the device. As shown in the graph, the device moves into the saturation region at about VDS = 0.6 V, beyond which the drain current stabilizes. This behavior is indicative of efficient channel pinch and strong gate modulation, validating the high-performance operation of the proposed HEMT structure.

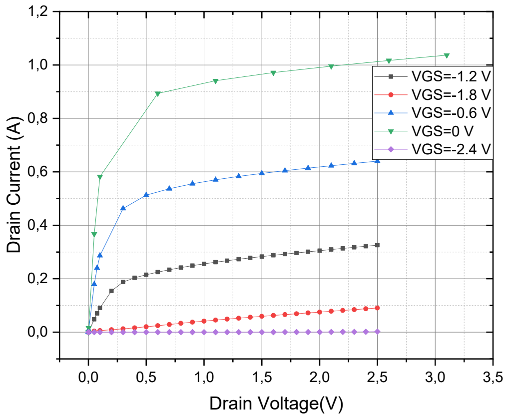

Figure 2: Family of IDS-VDS curves of the proposed AlGaN/GaN HEMT at different VGS values.

Figure 3 shows the simulated curve of the transfer characteristics (IDS–VGS) of the HEMT studied. During this simulation, the gate voltage is swept from −4 V to 0.5 V, while the drain voltage is held constant at 3 V. Analysis of the curve identifies a threshold voltage of around −2.5 V, corresponding to the value of VGS at which the drain current starts to grow rapidly from a near-zero level. This transition marks the transition of the device from the cut-off state to the active region of operation. The device channel, indicating efficient transport of the carriers in the structure. Such transconductance is particularly advantageous for radio frequency applications, where gain and switching speed are crucial.demonstrates a maximum transconductance of 698 ms/mm, extracted from the maximum slope

Journal of Information Systems Engineering and Management
2025, 10(4)
e-ISSN: 2468-4376
https://www.jisem-journal.com/
Research Article

of the IDS–VGS curve. This high value testifies to an efficient electrostatic coupling between the grid and the

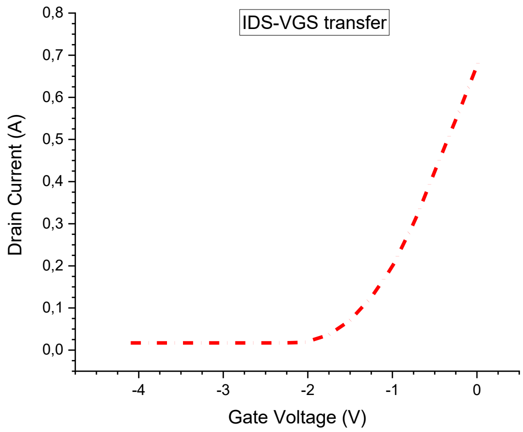

Figure 3. Transfer characteristics of the proposed Tshaped AlGaN/GaN HEMT at VDS= 3 V.

Figure 4 shows the transconductance (gm) curve extracted from the transfer characteristics of the simulated HEMT. This curve highlights the evolution of transconductance as a function of gate voltage (VGS), thus providing a fine evaluation of the dynamic behavior of the device. A gradual increase in transconductance is observed as the gate voltage becomes less negative, reaching a peak of 698 mS/mm around VGS = −1 V. This maximum value corresponds to the optimal amplification area of the device, where the modulation of the drain current by the gate voltage is most efficient. Beyond this point, a decrease in gm is noted, reflecting a progressive saturation of the canal or a reduced mobility effect due to the accumulation of carriers. This behavior is typical of transistors with high electron mobility, and reflects the balance between modulation efficiency and limitations related to carrier density and saturation velocity. The analysis of this curve confirms the excellent dynamic performance of the proposed structure. High, well-defined transconductance in a narrow range of gate voltage is a key indicator of linearity, high gain, and fast response capability—essential characteristics for RF amplifier circuits, high-frequency switches, and high-speed logic devices.

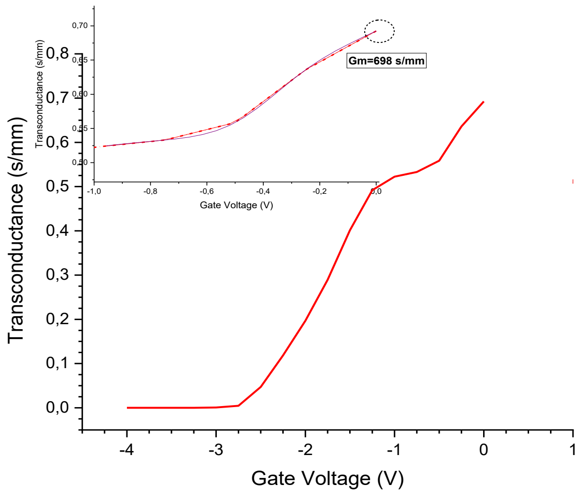

Figure 4: Evolution of transconductance (g_m) as a function of gate

Journal of Information Systems Engineering and Management
2025, 10(4)
e-ISSN: 2468-4376
https://www.jisem-journal.com/

Research Article

voltage (V_{GS}) at V_{DS}= 3V.

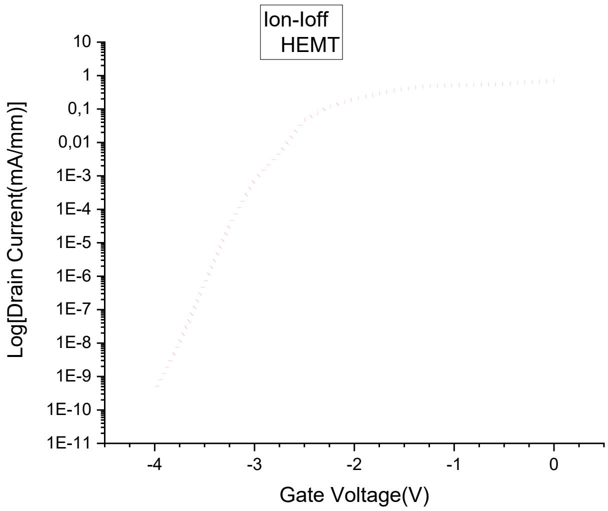

Figure 5: Semi-logarithmic plot of drain current (log I_{DS}) vs. gate-source voltage (V_{GS}) showing a subthreshold slope of 210 mV/decade at V_{DS} = 3 V.

Figure 5 illustrates the semi-logarithmic curve of the drain-source current (SDC) as a function of the gate-source voltage (VGS), obtained under a constant drain-source voltage of 3 V, at room temperature. This representation makes it possible to characterize the behavior of the device in the sub-threshold regime as well as to evaluate its switching performance. The simulation results reveal an on-state current (Ion) of 0.65 A and a blocked-state leakage current (Ioff) of 9.5×10^{-9} A, leading to an Ion/Ioff ratio of the order of 6.82×10^{7}. This high ratio is a testament to the transistor's ability to provide efficient isolation in OFF mode while maintaining high conductivity in ON mode, which is fundamental for high-performance devices in the fields of power electronics and radio frequency communications. The subthreshold swing (SS) is extracted from the linear region of the log(ID)–VGS curve, close to the threshold voltage. It represents the minimum variation in the VGS voltage necessary to reduce the IDS current by a decade (factor 10). Expressed in mV/decade, this quantity is a key indicator of the transistor's dynamic behavior, especially for low-power applications. A reduced value of SS indicates a rapid transition between the OFF and ON states, which is highly desirable in high-density, low-supply voltage ICs.

$$SS = \Delta Vgs/\Delta log(Ids) = \Delta Vgs/dec \quad (1)$$

$$= [-3.18 + 2.97]\ V/dec$$

$$= 210\ mV/decade$$

Microwave simulations are critical for evaluating the high-frequency performance of heterojunction field-effect transistors (HFETs). Two key parameters are commonly analyzed: the cut-off frequency (fT) and the maximum oscillation frequency (fmax) [28]. Gate leakage current is a pivotal factor in assessing device reliability and energy efficiency, particularly in the off-state. In an ideal device, this current is zero; however, in practical structures, it depends on the intrinsic quality of the semiconductor materials,

Journal of Information Systems Engineering and Management
2025, 10(4)
e-ISSN: 2468-4376
https://www.jisem-journal.com/
Research Article

the properties of the metal–semiconductor junction (notably Schottky contacts), and the gate architecture.

Figure 6 illustrates the gate leakage current as a function of gate–source voltage (VGS) at room temperature, with a fixed drain–source voltage of VDS = 3 V. The device exhibits an exceptionally low minimum leakage current of 2×10^{-11} A at VGS = 0.05 V and a maximum of 9×10^{-7} A at VGS = −0.25 V. Notably, even at an extreme negative gate bias of VGS = −4.0 V, the leakage current remains stable at 2×10^{-11} A. This outstanding electrical insulation and minimal power consumption at zero bias highlight the device's suitability for high-frequency applications, low heat dissipation, and high-reliability systems, such as next-generation communication technologies and energy-efficient electronic architectures.

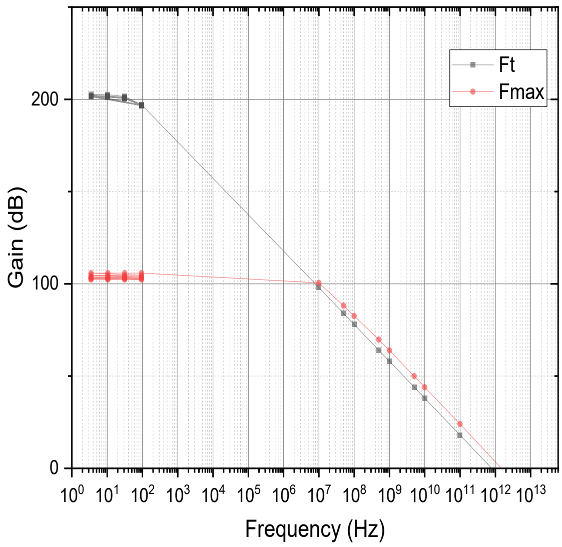

Figure 6: Current gain (fT) and power gain (fmax) vs. frequency at VDS = 3 V, VGS = 0 V

$$f_t \simeq \frac{g_m}{2\pi\,(C_{gs}+C_{gd})} \quad (1)$$

$$f_{max} \simeq \frac{f_t}{\sqrt{R_i g_{ds}}} \quad (2)$$

The microwave performance of HEMTs is significantly influenced by key internal parameters, including gate-drain capacitance (Cgd), gate-source capacitance (Cgs), channel resistance (Rch), and output conductance (Gds). These parameters critically govern the high-frequency behavior of the device. Specifically, the transition frequency (fT) and maximum oscillation frequency (fmax) serve as essential metrics for evaluating the transistor's suitability for radio-frequency (RF) circuits. The transition frequency (fT) represents the frequency at which the current gain drops to unity, while the maximum oscillation frequency (fmax) indicates the frequency at which the power gain becomes unity, both of

Journal of Information Systems Engineering and Management
2025, 10(4)
e-ISSN: 2468-4376
https://www.jisem-journal.com/
Research Article

which are pivotal for high-frequency applications. Figure 8 depicts the variation of fT and fmax for the proposed HEMT, illustrating its potential for efficient operation in RF and microwave circuits.

This study achieved a maximum current gain (|H21|) of 205 dB and a maximum power gain of 110 dB for an AlGaN/GaN HEMT with an AlGaN channel and T-shaped gate geometry. The simulated device exhibits a transition frequency (fT) of 748 GHz and a maximum oscillation frequency (fmax) of 1068.8 GHz under bias conditions of VGS = 0 V and VDS = 1.0 V, demonstrating exceptional potential for ultra-high-frequency telecommunications applications. Table 2 compares the electrical performance of the proposed HEMT with prior studies. Fabricated on a 4H-SiC substrate, this device significantly outperforms equivalents on silicon or sapphire substrates. The threshold voltage of −2.5 V is notably less negative than the −5.9 V and −4.0 V reported by Mura [1] and Chatterjee [28], respectively, reducing the gate voltage required for channel activation. Additionally, the maximum drain current reaches 0.987 A at VGS = 0 V, an order of magnitude higher than the 15 mA and 58 mA reported in [1] and [28]. The device also features a subthreshold slope of 0.210 V/decade, indicating a sharp transition between ON and OFF states and reduced leakage losses. Furthermore, a transconductance of 698 mS reflects superior drain current sensitivity to gate voltage and enhanced electron transport dynamics, surpassing the 260 mS and 122.5 mS reported in [1] and [28].

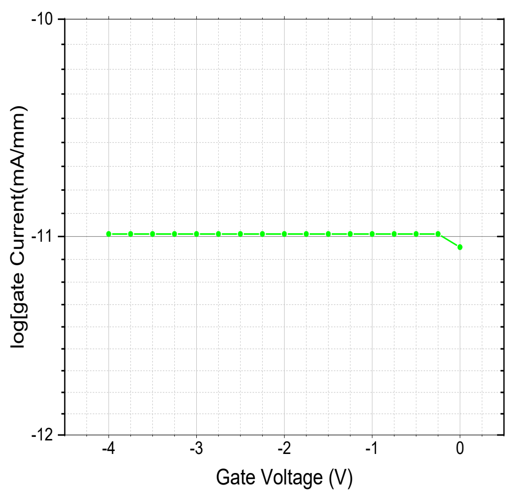

Figure 6: Gate leakage current (IGS) vs. gate-source voltage (VGS) at VDS = 3 V

Table 2: Comparison between this work and previous works.

Parameter	Mura [1]	Chatterjee [28]	This Work
Substrate	Silicon	Sapphire	4H-SiC
Gate Voltage Range	0 to 25 V	0 to 25 V	0 to 25 V
Threshold Voltage	−5.9 V	−4.0 V	−2.5 V
Maximum Drain Current	15 mA @ V_{GS} = 2 V	58 mA @ V_{GS} = 0 V	0.987 A @ V_{GS} = 0 V
Subthreshold Slope	0.220 V/dec	0.185 V/dec	0.210 V/dec
Transconductance	260 mS	122.5 mS	698 mS
Cut-off Frequency (f_T)	63 GHz	73.6 GHz	748 GHz

Journal of Information Systems Engineering and Management
2025, 10(4)
e-ISSN: 2468-4376
https://www.jisem-journal.com/

Research Article

CONCLUSION

This study demonstrates the superior electrical performance of an AlGaN/GaN HEMT with a T-shaped gate, simulated on a 4H-SiC substrate using Silvaco ATLAS. The advanced design, featuring a 20 nm gate length and double delta-doped AlGaN barriers, achieves a maximum drain current of 987.42 mA/mm, a transconductance of 698 mS/mm, a cut-off frequency (fT) of 748 GHz, and a maximum oscillation frequency (fmax) of 1068.8 GHz. A subthreshold slope of 210 mV/decade and a gate leakage current of 2 × 10-11 A ensure rapid switching and minimal power loss, while an Ion/Ioff ratio of 6.82 × 107 supports high-density integration. The combination of double delta doping, a high-mobility channel, and the high thermal conductivity of 4H-SiC positions this HEMT as a leading candidate for power electronics, 5G base stations, and low-power, ultrafast logic circuits. Future work will focus on experimental validation and scalability of the proposed design.

REFRENCES

[1] K. Murase, T. Akiyama, H. Takagi, Y. Takada, and S. Yamasaki, “T-shaped Gate GaN HFETs on Si with Improved Breaking Voltage and fmax,” IEEE Electron Device Lett., vol. 35, no. 5, pp. 524–526, May 2014. doi: 10.1109/LED.2014.2308313

[2] A. Douara, B. Djellouli, A. Rabehi, A. Ziane, and N. Belkadi, “IV Features Model for AlGaN/GaN HEMTs using TCAD-Silvaco,” J. New Technol. Mater., vol. 4, no. 2, pp. 16–24, 2014,doi: 10.12816/0010326 .

[3] A. Douara, N. Kermas, and B. Djellouli, “Capacitance models of AlGaN/GaN high electron mobility transistors,” Int. J. Nucl. Quantum Eng., vol. 10, no. 3, pp. 420–423, 2016., doi: 10.5281/zenodo.1123731

[4] A. Douara, B. Djellouli, H. Abid, A. Rabehi, A. Ziane, M. Mostefaoui, and N. Dif, “Optimization of the two-dimensional characteristics of electron gas of AlGaN/GaN high electron mobility transistors,” Int. J. Numer. Model. Electron. Netw. Devices Fields, vol. 32, no. 2, pp. e2518, 2019, doi: 10.1002/jnm.2518 .

[5] S. Prasad and A. K. Das, “Characterization of AlGaN/GaN and AlGaN/AlN/GaN HEMTs in terms of mobility and subthreshold slope,” J. Comput. Electron., vol. 15, no. 1, pp. 172–180, 2016, doi: 10.1007/s10825-015-0751-8,

[6] G. Parish et al., “AlGaN/AlN/GaN High Electron Mobility Transistors with Improved Carrier Transport,” in Proc. Conf. Optoelectron. Microelectron. Mater. Devices, Queensland, Australia, 2004, pp. 29–32, doi: 10.1109/COMMAD.2004.1577484.

[7] A. Douara, A. Rabehi, B. Djellouli, A. Ziane, and H. Abid, “2D optimization of current-voltage characteristics in AlGaN/GaN HEMTs with passivation layer influence,” Int. Rev. Ambient Energy, vol. 42, no. 12, pp. 1363–1366, 2021, doi: 10.1080/01430750.2019.1608856.

[8] X. Wang et al., “Effect of GaN Channel Layer Thickness on DC and RF Performance of GaN HEMTs with AlGaN/GaN Composite Buffer,” IEEE Trans. Electron Devices, vol. 61, no. 5, pp. 1341–1346, May 2014, doi: 10.1109/TED.2014.2312232

[9] S. Liu et al., “Al_2O_3/AlN/GaN MOS-Channel-HEMTs with an AlN Interfacial Layer,” IEEE Electron Device Lett., vol. 35, no. 7, pp. 723–725, Jul. 2014., doi: 10.1109/LED.2014.2322379.

[10] A. Douara, A. Rabehi, and M. Hamdani, “Effect of the geometric and physical parameters of the AlGaN/GaN HEMT on the electrical characteristics with the AlN spacer layer,” Int. J. Adv. Stud. Comput. Sci. Sci. Eng., vol. 11, no. 12, pp. 1–9, 2022., doi: .

Journal of Information Systems Engineering and Management
2025, 10(4)
e-ISSN: 2468-4376
https://www.jisem-journal.com/
Research Article

[11] L. Shen et al., “AlGaN/AlN/GaN high-power HEMT microwave,” IEEE Electron Device Lett., vol. 22, no. 10, pp. 457–459, Oct. 2001, doi: 10.1109/55.954910.

[12] A. Douara, A. Rabehi, O. Baitiche, and M. Hamdani, “Improvement of the electrical characteristics of the AlxGa1−xN/GaN high-mobility electron transistor by the effect of physical and geometric parameters,” Rev. Mex. Fis., vol. 69, no. 4, 2023. doi: 10.31349/RevMexFis.69.041001.

[13] K. H. Hamza, D. Nirmal, A. A. Fletcher, J. Ajayan, and R. Natarajan, “Improved drain current and cut-off frequency in the AlGaN/GaN HEMT with BGaN rear barrier,” Mater. Sci. Eng. B, vol. 284, p. 115863, 2022. doi: .

[14] R. Mohapatra and P. Dutta, “Improved transconductance and cut-off frequency in the high-electron mobility 0.3Ga0.7N/GaN dual-channel Al transistor by improving the contact length ratio of the drain source,” Pramana, vol. 94, no. 1, p. 5, 2020, doi:

[15] A. Douara, A. Rabehi, and O. Baitiche, “Impact of the AlN interlayer on the electronic and IV characteristics of In0.17Al0.83N/GaN HEMT,” Rev. Mex. Fis., vol. 69, no. 3, pp. 0–0, 2023.doi:10.31349/revmexfis.69.031602.

[16] A. Ziane et al., “Numerical investigation of G-V measurements of the GaAs metal-A nitride junction,” Rev. Mex. Fis., vol. 70, no. 6, pp. 061604-1, 2024, doi:10.31349/RevMexFis.70.061604.

[17] A. Rabehi et al., “Current-Voltage, Capacitance-Voltage-Temperature and DLTS Studies of Ni/6 Schottky H-SiC diode,” Semiconductors, vol. 55, no. 4, pp. 446–454, 2021, doi: 10.21883/FTP.2021.04.50744.9541A.

[18] R. Brown, A new high-mobility electron transistor in AlGaN/GaN-based enhancement mode with subcritical barrier thickness, Ph.D. dissertation, Univ. Glasgow, 2015., doi: 10.4028/p-t622l2.

[19] C. Leurquin, “Study of the degradation mechanisms and dynamic reliability of the GaN on Si devices,” Ph.D. dissertation, Univ. Grenoble Alpes, 2024.

[20] A. Rabehi et al., “Optimal estimation of Schottky diode parameters using advanced swarm intelligence algorithms,” Semiconductors, vol. 54, pp. 1398–1405, 2020,doi: 10.1134/S1063782620110214.

[21] J. W. Chung, W. E. Hoke, E. M. Chumbes, and T. Palacios, “AlGaN/GaN HEMT with 300 GHz fmax,” IEEE Electron Device Lett., vol. 31, no. 3, pp. 195–197, 2010,doi: 10.1109/LED.2009.2038935.

[22] M. Haziq et al., “Challenges and Opportunities for High-Power, High-Frequency AlGaN/GaN High Electronic Mobility Transistor (HEMT) Applications: A Review,” Micromachines, vol. 13, no. 12, p. 2133, 2022,doi: 10.3390/mi13122133.

[23] S. K. Dubey, M. Mishra, and A. Islam, “Characterization of AlGaN/GaN-based HEMTs for low-noise, high-frequency applications,” Int. J. Numer. Model., vol. 35, no. 1, p. e2932, 2022,doi:10.1002/jnm.2932.

[24] A. Schenk, “An improved approach to Shockley-Read-Hall recombination in inhomogeneous fields of spatial charge regions,” J. Appl. Phys., vol. 71, no. 7, pp. 3339–3349, 1992,doi: 10.1063/1.350929.

[25] T. Nakamura et al., “Reduction of Shockley-Read-Hall recombination losses in the depletion region of a solar cell using a wide-gap emitter layer,” J. Appl. Phys., vol. 130, no. 15, 2021,doi: 10.1063/5.0060158.

[26] M. Sotoodeh, A. H. Khalid, and A. A. Rezazadeh, “Empirical low-field mobility model for III-V compounds applicable in device simulation codes,” J. Appl. Phys., vol. 87, no. 6, pp. 2890–2900, 2000,doi: 10.1063/1.372274.

[27] C. S. Rafferty, M. R. Pinto, and R. W. Dutton, “Iterative methods in the simulation of semiconductor devices,” IEEE Trans. Electron Devices, vol. 32, no. 10, pp. 2018–2027, 1985,doi: 10.1109/TCAD.1985.1270144.

Journal of Information Systems Engineering and Management
2025, 10(4)
e-ISSN: 2468-4376
https://www.jisem-journal.com/

Research Article

[28] M. Cmeliani, Micro and Nanotechnologies Microelectronics, Paris VII, Univ. Paris Diderot, 2003.
[29] S. Chatterjee, A. Sengupta, S. Kundu, and A. Islam, "Analysis of the AlGaN/GaN high-mobility transistor for high-frequency application," in Proc. DevIC 2017: Devices for Integrated Circuit, pp. 196–199, 2017,doi: 10.1109/DEVIC.2017.8073935.